

Abstract

Integrating nephelometers are instruments that directly measure a value close to the light scattering coefficient of airborne particles. Different models of nephelometers have been used for decades for monitoring and research applications. Now, a series of nephelometers (Ecotech models M9003, Aurora 1000 and Aurora 3000) with newly designed light sources based on light emitting diodes are available. This article reports on the design of these integrating nephelometers and a comparison of the Aurora 3000 to another commercial instrument (TSI model 3563) that uses an incandescent lamp. Both instruments are three-wavelength, total and backscatter integrating nephelometers.

We present a characterization of the new light source design of the Aurora 3000 and provide parameterizations for its angular sensitivity functions. These parameterizations facilitate to correct for measurement artefacts using Mie-theory. Comparison measurements against the TSI 3563 with laboratory generated white particles and ambient air are shown and discussed. Both instruments agree well within the calibration uncertainties and detection limit for total scattering with differences less than 5%. Differences for backscattering are higher by up to 11%. Highest differences were found for the longest wavelengths, where the signal to noise ratio is lowest. Differences at the blue and green wavelengths are less than 4% and 3%, respectively, for both total and backscattering.

1 Introduction

Integrating nephelometers, first introduced by Beuttell and Brewer (1949), offer a method of measuring the light scattering coefficient of airborne particles. Because no assumptions about particle composition, size or shape are necessary, the use of integrating nephelometers is widespread for ambient air monitoring as well as for laboratory studies. A scientific review of this type of instrument was given by Heintzenberg

AMTD

3, 4835–4864, 2010

Three-wavelength LED-based total scatter integrating nephelometer

T. Müller et al.

Title Page

Abstract

Introduction

Conclusions

References

Tables

Figures

⏪

⏩

◀

▶

Back

Close

Full Screen / Esc

Printer-friendly Version

Interactive Discussion



and Charlson (1996). Integrating nephelometers can be calibrated with gases of well know scattering coefficients, which facilitates quality assurance and maintenance.

Radiative transfer calculations of the Earth's atmosphere require the scattering phase function or at least the asymmetry parameter of airborne particles. One method of estimating the asymmetry parameter is to convert the measured back scatter fraction, the ratio of hemispheric backscattering to total scattering, into their corresponding asymmetry parameters. Integrating nephelometry for measuring hemispheric backscattering is described in Charlson et al. (1974) and Heintzenberg (1978), and relationships between backscatter fraction and particle asymmetry parameter were investigated by Marshall et al. (1995) and Andrews et al. (2006).

Several studies on the performance of integrating nephelometers (Anderson et al., 1996; Heintzenberg et al., 2006; Müller et al., 2009; Massoli et al., 2009) were performed. Previous intercomparisons of instruments of different makes are limited to total scattering only. We present the first intercomparison of two integrating total/backscatter nephelometers. Additionally to the backscatter option both nephelometers are three wavelength instruments. One instrument type TSI 3565 (model 3563, TSI Inc, St. Paul, MN, USA) was characterized in detail by Anderson et al. (1996). In the recent years nephelometers (models M9003, Aurora 1000, and Aurora 3000) with light emitting diodes were developed by Ecotech Pty, Ltd, Knoxfield, Australia.

We present the history of development of the Ecotech Aurora 3000 integrating nephelometer and a comparison of this three wavelength total and backscattering instrument against the TSI model 3565. We discuss the theory of integrating nephelometers and describe the Aurora 3000 instrument. Furthermore, we investigate the characteristic of the angular sensitivity of the new light source design. Finally, intercomparison experiments between the two integrating nephelometer types are presented and discussed using ammonium sulfate and ambient aerosols.

Three-wavelength LED-based total scatter integrating nephelometer

T. Müller et al.

Title Page

Abstract

Introduction

Conclusions

References

Tables

Figures



Back

Close

Full Screen / Esc

Printer-friendly Version

Interactive Discussion



2 Principle of operation of integrating nephelometers and instruments descriptions

2.1 Theory of integrating nephelometers

The total scattering signal $S_{ts,\lambda}$ and hemispheric backscattering signal $S_{bs,\lambda}$ measured by integrating nephelometers at wavelength λ can be written as

$$S_{ts,\lambda} = \int_0^{180} F_\lambda(\theta) Z_{ts}(\theta) d\theta \quad (1)$$

and

$$S_{bs,\lambda} = \int_0^{180} F_\lambda(\theta) Z_{bs}(\theta) d\theta, \quad (2)$$

where $Z_{ts}(\theta)$ and $Z_{bs}(\theta)$ are the angular sensitivity functions of the nephelometer for total scattering and backscattering, respectively, and θ is the scattering angle.

$$F_\lambda(\theta) = \int_{-\infty}^{+\infty} f_\lambda(\theta, m_\lambda, d_p) \frac{dn(d_p)}{d \log d_p} \pi \left(\frac{d_p}{2}\right)^2 d \log d_p + F_R(\theta) \quad (3)$$

is the angular scattering function of the particle population and the carrier gas. The particle number size distribution is given by $dn(d_p)/d \log d_p$ and $f_\lambda(\theta, m_\lambda, d_p)$ is the angular scattering function of the individual particles with complex refractive index m_λ and diameter d_p . f_λ can be calculated using scattering codes. For calculations throughout the manuscript, a code given in Bohren and Huffman (1983) was used. $F_R(\theta)$ is the contribution of the Rayleigh scattering of the carrier gas to the scattering function. Calibration of integrating nephelometers with two particle free gases of known

Three-wavelength LED-based total scatter integrating nephelometer

T. Müller et al.

Title Page

Abstract

Introduction

Conclusions

References

Tables

Figures

⏪

⏩

◀

▶

Back

Close

Full Screen / Esc

Printer-friendly Version

Interactive Discussion

Rayleigh scattering coefficients yields calibration constants K which relate the scattering signals S to the total scattering (subscript ts) and backscattering (subscript bs) coefficients by

$$\sigma_{ts,\lambda} = K_{ts,\lambda} S_{ts,\lambda} - \sigma_{tsR,\lambda} \quad (4)$$

and

$$\sigma_{bs,\lambda} = K_{bs,\lambda} S_{bs,\lambda} - \sigma_{bsR,\lambda} \quad (5)$$

where the contribution for Rayleigh scattering $\sigma_{tsR,\lambda}$ and $\sigma_{bsR,\lambda}$ are calculated analytically (e.g. Buchholz, 1995) for given temperature and pressure and subtracted from the scatter signals.

Angular sensitivity functions of an ideal nephelometer would be

$$Z_{ts}(\theta) = \sin(\theta) \quad (6)$$

for total scattering and

$$Z_{bs}(\theta) = \begin{cases} \sin(\theta) & 90 < \theta < 180 \\ 0 & \text{otherwise} \end{cases} \quad (7)$$

for backscattering. The calculated coefficients (Eqs. 1 to 7) are denoted as *true total scattering coefficient* $\sigma_{ts}^{\text{true}}$ and *true backscattering coefficient* $\sigma_{bs}^{\text{true}}$ for ideal angular sensitivity functions. The angular sensitivity functions of nephelometers are formed by a light source with Lambertian radiant emission meaning that the angular illumination of the particles is almost a sin-function. In the backscattering mode, a shutter prevents forward emitted light from reaching the sample volume. Because illumination functions of integrating nephelometers deviate little from a sin-function (Anderson et al., 1996; Müller et al., 2009), and due to a limited range of angular integration (e.g. Anderson et al., 1996; Moosmüller et al., 2003), integrating nephelometers measure the so called *nephelometer total scattering* $\sigma_{ts}^{\text{neph}}$ and *nephelometer backscattering* $\sigma_{bs}^{\text{neph}}$. In the following, the term *angular sensitivity* comprises both the non-Lambertian illumination

Three-wavelength LED-based total scatter integrating nephelometer

T. Müller et al.

Title Page

Abstract

Introduction

Conclusions

References

Tables

Figures

◀

▶

◀

▶

Back

Close

Full Screen / Esc

Printer-friendly Version

Interactive Discussion



and the angular truncation. We follow the definition of correction factors from Anderson and Ogren (1998), where the ratios of *true* to measured *nephelometer* values for both total scattering and backscattering are defined by

$$C_{ts,\lambda} = \frac{\sigma_{ts,\lambda}^{true}}{\sigma_{ts,\lambda}^{neph}} \frac{\sigma_{tsR,\lambda}^{neph}}{\sigma_{tsR,\lambda}^{true}} \quad (8)$$

5 and

$$C_{bs,\lambda} = \frac{\sigma_{bs,\lambda}^{true}}{\sigma_{bs,\lambda}^{neph}} \frac{\sigma_{bsR,\lambda}^{neph}}{\sigma_{bsR,\lambda}^{true}}, \quad (9)$$

respectively. The second quotients in the above equations compensate for the non-ideal illumination function, when calibrating the nephelometer with Rayleigh scattering gases. The correction factors $C_{ts,\lambda}$ and $C_{bs,\lambda}$ depend on both particle size and refractive index. If angular sensitivity functions $Z_{ts}(\theta)$ and $Z_{bs}(\theta)$ are known, correction factors can be simulated for given particle number size distributions and refractive indices. Easy to use parameterizations for sensitivity functions are given in Sect. 3.

2.2 Instrument descriptions

2.2.1 Development of the Ecotech model Aurora 3000 integrating nephelometer

15 In 2002, the first LED (light emitting diode) based nephelometer with type designation M9003 was developed by Ecotech. The unique feature of this nephelometer was an array of seven LEDs, where the LEDs were shining to the center point of a diffusing plate. The electrical drive current of each LED was adjusted so that the angular intensity distribution of the light source was nearly a Lambertian radiation distribution. The
 20 M9003 nephelometer was a single wavelength total scatter only nephelometer. The nephelometer was available at wavelengths of 470, 525, or 630 nm. The performance

Three-wavelength LED-based total scatter integrating nephelometer

T. Müller et al.

Title Page

Abstract

Introduction

Conclusions

References

Tables

Figures

⏪

⏩

◀

▶

Back

Close

Full Screen / Esc

Printer-friendly Version

Interactive Discussion



Three-wavelength LED-based total scatter integrating nephelometer

T. Müller et al.

Title Page

Abstract

Introduction

Conclusions

References

Tables

Figures

⏪

⏩

◀

▶

Back

Close

Full Screen / Esc

Printer-friendly Version

Interactive Discussion



of the M9003 with wavelength 525 nm was investigated during nephelometer intercomparisons and calibration workshops (Heintzenberg et al., 2006; Müller et al., 2009). An improvement of the performance of the illumination function was achieved by using 15 LEDs and released as model Aurora 1000. A new three-wavelength light source (used in the original Aurora 3000 model nephelometers) was designed which included 3 light source boards in one housing with a total of 45 LEDs. In all cases, LEDs of different colours are sequentially switched on and off and allowing detection of scattering signals at all three wavelengths with a single photomultiplier tube. A recalibration of the brightness of each LED in models M9003, Aurora 1000, and Aurora 3000 was time-consuming and cannot be done by the user. It is known that an optically thicker opal glass diffuser helps to form a Lambertian illumination function. However, an opal glass reduces the transmitted intensity. With rapid improvements in LED technology, it has become possible to obtain higher intensity outputs from smaller LED packages. Ecotech released an opal glass LED light source in November 2008. This light source utilizes an opal glass diffuser fitted in front of a small array of only 3 high intensity LEDs per wavelength to form a Lambertian distribution. The light source is attached to the sensing volume. The angular integration of nephelometers is limited by apertures at both ends of the sensing volume. For the Aurora 3000 and 1000 the angular integration ranges from 10° to 171° .

A further development of the Aurora 3000 was to implement a hemispheric backscatter mode. A motor driven backscatter shutter, which is attached to the light source block, moves periodically between two pre-programmed positions. Sketches of the nephelometer cell, light source, and backscatter shutter are given in Fig. 1. The position of the shutter is controlled by a servomotor with position feedback, a servo controller (mounted on the outside of the light source) and the microprocessor. In the backscatter position, the shutter blocks the light emitted in forward direction. The remaining scattered light is seen by the detector as hemispheric backscattering.

2.2.2 TSI model 3563

For comparison purposes, the integrating nephelometer model TSI 3563 was also used in this study. For a detailed description of the TSI 3563, we refer to Anderson et al. (1996). We briefly summarize the main parameters of interest. The light source of the model 3563 is an incandescent quartz-halogen lamp, which emits light in a large range of wavelengths. An elliptical mirror focuses light onto one end of an optical pipe. The other end of the pipe is attached to an opal glass diffuser providing a nearly Lambertian emission. In the forward scattering direction, an aperture limits the angular integration to angles greater than 7° . At the other side, a shadow plate limits the integration to angles less than 170° . Light scattered by particles enters the detection unit and is split by dichroic filters into three light beams of different spectral ranges. Interference filters in the light beams limit the spectral transmittance to a well-defined wavelength range of about 40 nm before the light is detected by photomultiplier tubes. A rotating backscatter shutter blade periodically blocks light emitted in the forward direction and thus allows measurement of the hemispheric backscatter signal.

3 Angular illumination functions

Angular illumination functions for TSI 3563 were measured in a previous study (Müller et al., 2009) with a goniometer setup. For this study, illumination functions for the Aurora 3000 were measured using the same experimental setup with small modifications. We briefly describe here the principle of the angular intensity measurements.

The light source of the Aurora 3000 was removed and mounted on an optical bench in the centre of a computer controlled rotating arm. Relative emitted intensity was measured with detection optics at the end the rotating arm at angles $0^\circ < \theta < 180^\circ$ in steps of 5° . The detection optics consists of a lens which couples the light into an optical fibre and a photodiode attached to the other end of the fibre. Before measuring, it was ensured that the field of view of the detection optics was large enough to cover

Three-wavelength LED-based total scatter integrating nephelometer

T. Müller et al.

Title Page

Abstract

Introduction

Conclusions

References

Tables

Figures



Back

Close

Full Screen / Esc

Printer-friendly Version

Interactive Discussion



the whole surface of the opal glass of the light source. The overall angular alignment was estimated to be less than one degree.

Measured angular intensity functions for the Aurora 3000 are shown in Fig. 2. Wavelengths are indicated by B (450 nm), G (525 nm), and R (635 nm), respectively, and total scattering and backscattering are indicated by t_s and b_s , respectively. Total scattering illumination functions were normalized to unity at a scattering angle of 90° and the backward scattering illumination function was adjusted to match the value of the total scattering illumination function at 110° . Illumination functions for total scattering and for backscattering agree well among each other at large scattering angles ($\theta > 110^\circ$).

Illumination functions of TSI 3563 were measured independently and published in Anderson et al. (1996) and Müller et al. (2009). The illumination functions measured in those studies agreed well. It also was found, that there is no difference between illumination functions for different nephelometer wavelengths.

Beside the non-Lambertian illumination, the angular truncation contributes to the overall angular sensitivity function. Truncation angles for the TSI 3563 were given in Anderson et al. (1996) and were reported to be 7° and 170° . From technical drawings truncation angles for the Aurora 3000 were determined to be 10° and 171° . To our knowledge there is currently no experimental verification method for estimating truncation angles.

A parameterization was developed for total and backscattering sensitivity functions. The parameterizations are modifications of sin-functions with

$$Z_{t_s}(\theta) = \begin{cases} 0 & 0^\circ \leq \theta \leq \alpha_1 \\ \beta_1 \cdot \sin(\theta)^{\beta_2} & \alpha_1 < \theta < \alpha_2 \\ 0 & \alpha_2 \leq \theta \leq 180^\circ \end{cases} \quad (10)$$

and

$$Z_{b_s}(\theta) = \begin{cases} 0 & 0^\circ \leq \theta \leq \alpha_1 \\ \max\left(0, \beta_1 \cdot \sin(\theta)^{\beta_2} \cdot \min\left(0, \frac{\theta - \gamma_1}{\gamma_2}\right)\right) & \alpha_1 < \theta < \alpha_2 \\ 0 & \alpha_2 \leq \theta \leq 180^\circ \end{cases} \quad (11)$$

Three-wavelength LED-based total scatter integrating nephelometer

T. Müller et al.

Title Page

Abstract

Introduction

Conclusions

References

Tables

Figures

⏪

⏩

◀

▶

Back

Close

Full Screen / Esc

Printer-friendly Version

Interactive Discussion



Three-wavelength LED-based total scatter integrating nephelometer

T. Müller et al.

Title Page

Abstract

Introduction

Conclusions

References

Tables

Figures

⏪

⏩

◀

▶

Back

Close

Full Screen / Esc

Printer-friendly Version

Interactive Discussion

where α_1 and α_2 account for the upper and lower truncation and β_2 accounts for the decreased relative illumination at small and large angles. β_1 is a scaling factor which cancels out (cf. Eqs. 8 and 9). The shadowing of the backscatter shutter is accounted for by parameters γ_1 and γ_2 . Parameters for TSI model 3565 and Aurora 3000 are given in Table 1. For comparison, Fig. 3 shows measured and parameterized illumination functions.

Correction factors for angular sensitivity (truncation and illumination) were calculated for the TSI 3565 and Aurora 3000 and are shown in Fig. 4 versus the volume median diameter of a lognormal volume size distribution with geometric standard deviation 1.6. The refractive index was chosen to be $1.53-0.01i$, what corresponds to a weakly absorbing aerosol. Corrections factors were calculated using Eqs. (8) and (9) with the parameterizations given in Eqs. (10) and (11) and the corresponding parameters given in Table 1. The wavelengths were 525 nm and 550 nm for the Aurora 3000 and TSI 3563, respectively. For total scattering the correction factor increases for larger diameters and correction factors for the Aurora 3000 are higher than the corresponding values of the TSI 3563. The reason for this is the larger truncation angle in the forward scattering direction. The backscattering correction factors are smaller compared to total scattering with differences between the Aurora 3000 and TSI 3563 of less than 2%.

4 Instrument characterization

4.1 Noise and detection limit

Noise levels and detection limits were investigated in Anderson et al. (1996) for the TSI 3565. At low particle concentrations or short sampling times, the dominant source of uncertainties is random noise. The detection limit was defined as a signal to noise ratio of 2 and was given to be 0.2 and 0.1 Mm^{-1} for total scattering and backscattering, respectively, at 550 nm and 5 min averaging time. For the Ecotech Aurora 3000, the noise was determined when sampling filtered air. The detection limits with a one minute

measured with an optical particle size spectrometer (UHSAS, Droplet Measurement Technologies, Boulder, CO, USA). Particle size classification with optical spectrometers depends on the particles refractive index. Since refractive indices of ammonium sulphate and polystyrene latex, which was used for calibration of UHSAS, are known, size spectra were corrected to a volume equivalent particle diameter. Particle number size distributions were used to calculate correction factors for angular sensitivity functions. The volume median diameter was on average 0.24 μm with lower (10th percentile) and upper (90th percentile) diameters of 0.20 μm and 0.68 μm , respectively.

5.1.2 Instrument comparison

For comparison, scattering and backscattering coefficients measured by TSI 3563 were adjusted to wavelengths 450, 525 and 635 nm using the Ångström exponents defined by

$$\alpha_{\text{ts},\lambda_1,\lambda_2} = -\ln\left(\sigma_{\text{ts},\lambda_1}/\sigma_{\text{ts},\lambda_2}\right)/\ln\left(\lambda_1/\lambda_2\right). \quad (12)$$

and

$$\alpha_{\text{bs},\lambda_1,\lambda_2} = -\ln\left(\sigma_{\text{bs},\lambda_1}/\sigma_{\text{bs},\lambda_2}\right)/\ln\left(\lambda_1/\lambda_2\right). \quad (13)$$

Ångström exponents $\alpha_{\text{ts},\lambda_1,\lambda_2}$ and $\alpha_{\text{bs},\lambda_1,\lambda_2}$ are calculated from two pairs of scattering coefficients and wavelengths. Equations (12) and (13) can be used to adjust scattering and backscattering coefficients to any other wavelength in the interval $[\lambda_1, \lambda_2]$.

Scatter-plots of total and backscattering are shown in Fig. 5. Results of a linear regression analysis are summarized in Table 2a. After correction for the angular sensitivity, total scattering coefficients measured by the Ecotech Aurora 3000 and TSI 3563 differ between 2% and 5%. Differences in backscattering are between 1% and 11%. Differences for total scattering are in agreement with the uncertainties of calibration. The highest deviation occurs for the red channels in backscattering mode and can not be explained by calibration uncertainties. Both nephelometers have the lowest signal

Three-wavelength LED-based total scatter integrating nephelometer

T. Müller et al.

Title Page

Abstract

Introduction

Conclusions

References

Tables

Figures

⏪

⏩

◀

▶

Back

Close

Full Screen / Esc

Printer-friendly Version

Interactive Discussion



to noise ratios for this channel. The intercepts of all linear regressions are small and close to the sum of detection limits of both nephelometers.

A statistical analysis of Ångström exponents is given in Table 3. Ångström exponents for total scattering differ by 5% and 1% for wavelength pairs 450/525 and 525/635, respectively. Differences in backscattering are higher and amount 11% and 17% for the same wavelength pairs.

5.2 Ambient air

5.2.1 Setup and aerosol characterization

An ambient air intercomparison was performed for a period of 46 days in December 2009 and January 2010. The aerosol was fed through an aerosol inlet and Nafion™ membrane diffusion dryers (ANSYCO Inc., Karlsruhe, Germany) into a mixing chamber, which ensures equal aerosol concentrations at all output ports of the chamber. The aerosol was dried to a relative humidity of less than 25%. Transport losses through the inlet, Nafion dryer, mixing chamber and aerosol transport lines into the chamber are not specified. Transport losses from the chamber to the instruments were estimated to be small and did not affect the instrument comparison.

Particle number size distributions were measured with an SMPS (Scanning mobility particle sizer; Wang and Flagan, 1989) for mobility diameters d_m between 30 and 800 nm. Aerodynamic size spectra were measured with an APS (Aerodynamic particle sizer, model 3321, TSI Inc., St. Paul, MN) from aerodynamic diameters d_{aer} between 542 nm and 19.81 μm . The relations between mobility diameter, aerodynamic diameter and diameter of volume equivalent spheres d_{veq} are given by $d_{veq} = d_m / \chi$ for SMPS and $d_{veq} = d_{aer} / \sqrt{\rho / \chi}$ for APS, where ρ and χ are the particle density in units of g/cm^3 and the dynamic shape factor (e.g. DeCarlo et al., 2004), respectively. Because no information about the particle shape and density were available, the particles were considered to be spherical with a dynamic shape factor of unity and the particle density

Three-wavelength LED-based total scatter integrating nephelometer

T. Müller et al.

Title Page

Abstract

Introduction

Conclusions

References

Tables

Figures

◀

▶

◀

▶

Back

Close

Full Screen / Esc

Printer-friendly Version

Interactive Discussion



Three-wavelength LED-based total scatter integrating nephelometer

T. Müller et al.

Title Page

Abstract

Introduction

Conclusions

References

Tables

Figures

⏪

⏩

◀

▶

Back

Close

Full Screen / Esc

Printer-friendly Version

Interactive Discussion



was assumed to be 1.7 g/cm^3 , what roughly corresponds to ammonium sulfate. Size spectra from SMPS and APS were combined to a particle number size distribution, which was used to calculate volume size distributions $dV(d_p)/d \log d_p$ and volume median diameters D_{V_m} . For additional aerosol characterization, the particle absorption coefficient was measured with a MAAP (Multi angle absorption photometer, Thermo Fisher Scientific Inc., Waltham, USA).

Average volume size distributions for three ranges of volume median diameters are shown in Fig. 6. The particle volume concentration ranges between 1.5 and $60 \mu\text{m}^3/\text{m}^3$ and the range of volume median diameter is between 0.2 and about $0.48 \mu\text{m}$. Ambient air particles are a mixture of different compounds. An external mixing state means that individual particles consist of a single compound. In internally mixed aerosol, several compounds can be found in individual particles. The mixing is important when considering absorption whereas the scattering coefficient in contrast is less sensitive to the mixing state. Since we have no information about the mixing state, we assume an internally mixed aerosol with a size independent complex refractive index. This assumption might be supported by backward trajectories, which indicate that the air mass during the comparison measurements was an aged continental aerosol. The complex refractive index $m = n - ik$ was calculated by an iterative algorithm. Differences between simulated and measured scattering and absorption were minimized by optimizing the imaginary part of the refractive index until the minimization function $\zeta(k)$ defined by

$$\zeta(k) = \sqrt{\left(\frac{\sigma_{\text{ts},525\text{nm}}^{\text{neph}} - \sigma_{\text{ts},525\text{nm}}^{\text{Mie}}(k)}{\sigma_{\text{ts},525\text{nm}}^{\text{neph}}}\right)^2 + \left(\frac{\sigma_{\text{abs},637\text{nm}}^{\text{MAAP}} - \sigma_{\text{abs},637\text{nm}}^{\text{Mie}}(k)}{\sigma_{\text{abs},637\text{nm}}^{\text{MAAP}}}\right)^2} \quad (14)$$

has its minimal value. The measured and calculated values are indicated by upper indices neph and Mie respectively. The real part of the refractive index was chosen to be $n = 1.53$, a typical value for low absorbing ambient aerosol mainly consisting of ammonium sulphate (Wex et al., 2002). Minimization was done using the nephelometer scattering coefficient at 525 nm measured with the Aurora 3000 and the absorption

coefficient measured at 637 nm with the MAA. Mie-simulated scattering includes angular sensitivity corrections for the Aurora 3000 to simulate the measured nephelometer scattering.

5.2.2 Nephelometer comparison

5 Total scattering and backscattering coefficients measured by the Aurora 3000 and TSI 3563 were compared. Figure 7 shows angular sensitivity corrected scattering and backscattering at wavelengths 525 nm for both nephelometer models. There is an excellent agreement between both instruments with a coefficient of determination (R^2) higher than 0.99 for both total scattering and backscattering. Deviations in the slope are small with about 1% and 3% for total scattering and backscattering, respectively. Linear fit parameters for all three wavelengths and for uncorrected as well as corrected values are summarized in Table 2b. In all cases the coefficients of determination are better than 0.99. For uncorrected scattering, the slopes averaged for all three wavelengths are 0.96 and 1.02 for total scattering and backscattering, respectively. Average slopes after applying angular sensitivity correction corrections are 0.98 and 1.00. Differences in the slopes of the blue and green channels are less than 2%. Differences in the red wavelength compared to the other wavelengths are about 6%. Higher deviations in the red channels cannot be explained. Deviations in the slope for the blue and green channels are less than the uncertainties of calibration, showing that the instruments agree well within the specified uncertainties.

Measurements of Ångström exponents are often used for aerosol characterization. Changes of Ångström exponents indicate changes of the volume median diameter of the particle population, where a higher Ångström exponent indicates smaller volume median diameters. Also in Anderson and Ogren (1996) a correction of nephelometer truncation based on measured Ångström exponents was derived. We compared Ångström exponents derived from the Aurora 3000 and TSI 3563. Ratios of Ångström exponents (α_R), defined by Ångström exponents from the Aurora 3000 divided by Ångström exponents from the TSI 3565, were investigated. Figure 8 shows

Three-wavelength LED-based total scatter integrating nephelometer

T. Müller et al.

Title Page

Abstract

Introduction

Conclusions

References

Tables

Figures



Back

Close

Full Screen / Esc

Printer-friendly Version

Interactive Discussion



ratios of Ångström exponents versus the volume median diameter for total scattering and backscattering as well as for uncorrected and angular sensitivity corrected values. When considering total scattering, the slope of the regression line is significantly better for angular sensitivity corrected values. For backscattering the ratios of Ångström exponents are similar for the cases with and without angular sensitivity correction. The majority of volume median diameters was between 0.2 and 0.4 μm . In this range, the Ångström exponents with angular sensitivity correction differ between 3% and 11% for total scattering, with the TSI 3563 reading the higher values. For backscattering the Aurora is higher by 8% for the smaller volume median diameters and lower by 6% for the larger volume median diameters. The noise (standard deviation) of the ratios is 6% for total scattering. The noise for backscattering ratios is much higher with 28%, which can be explained by the much smaller signal to noise ratio for the backscatter signal compared to total scattering.

In all cases there is a tendency, that the ratio becomes smaller for larger volume median diameters. For corrected scattering and backscattering, this effect is less than for uncorrected scattering. It is unlikely that uncertainties of the gas calibration are responsible for the tendency. Faulty calibration factors at one or two wavelengths can cause a constant bias in the Ångström exponents but cannot explain the observed size dependence in the ratio of Ångström exponents. Possibly, truncation angles were not determined correctly for either one or both of the nephelometers, or truncation angles were not determined in exactly the same way. Unfortunately, there is no current experimental method for measuring the nephelometer angular sensitivity including angular truncation, illumination function, and the cell dimension in a single setup. This deficiency prevents a better characterization of nephelometers.

Three-wavelength LED-based total scatter integrating nephelometer

T. Müller et al.

[Title Page](#)[Abstract](#)[Introduction](#)[Conclusions](#)[References](#)[Tables](#)[Figures](#)[⏪](#)[⏩](#)[◀](#)[▶](#)[Back](#)[Close](#)[Full Screen / Esc](#)[Printer-friendly Version](#)[Interactive Discussion](#)

6 Summary

We presented the development of the new Ecotech Aurora 3000 integrating nephelometer. The Aurora 3000 is a three-wavelength total and backscatter integrating nephelometer. The light source consists of three LEDs per wavelength. An opal glass diffuser provides a nearly Lambertian angular illumination function, which is cut by the cell geometry at truncation angles of 10° and 171° . A periodically moving shutter allows measurement of hemispheric backscattering. An intercomparison of the Ecotech Aurora 3000 and the TSI 3563 three-wavelength total scatter and backscatter integrating nephelometers was performed in this investigation. To correct systematic uncertainties due to angular truncation and non-Lambertian illumination, truncation angles were obtained from technical drawings and angular illumination functions of the Ecotech Aurora 3000 were measured and compared to the TSI model 3563 nephelometer. The TSI model 3563 was previously characterized in detail by Anderson et al. (1996) and Müller et al. (2009). Parameterizations of angular sensitivities for total scattering and backscattering were derived for both models of nephelometers.

The Ecotech Aurora 3000 and TSI 3563 integrating nephelometers were compared using ammonium sulphate and ambient air. Scattering and backscattering coefficients at wavelengths 450 and 525 nm agree well within the calibration uncertainties. Calibration uncertainties are less than 3% and 5% for total and backscattering, respectively. Maximum differences in total scattering are 4% (450 nm), 2% (525 nm) and 5% (635 nm), when considering experiments with ambient air and laboratory generated white particles. For backscattering the differences are higher and amount to 7% (450 nm), 3% (525 nm) and 11% (635 nm). Ångström exponents for a large range of volume median diameters were investigated during an ambient air experiment. Ångström exponents derived at the wavelength pair 450 and 525 nm agree well with differences less than 5% for particle populations with volume median diameter less than $0.3\ \mu\text{m}$. Ratios of Ångström exponents for both nephelometer models show a slight dependence on volume median diameters. A sound explanation of this size

Three-wavelength LED-based total scatter integrating nephelometer

T. Müller et al.

Title Page

Abstract

Introduction

Conclusions

References

Tables

Figures

⏪

⏩

◀

▶

Back

Close

Full Screen / Esc

Printer-friendly Version

Interactive Discussion



effect is missing. However, values of scattering and backscattering coefficients of both nephelometers agree well.

Acknowledgements. The authors thank T. M. Tuch and A. Schladitz for their assistance during measurements.

References

Anderson, T. L. and Ogren, J. A.: Determining aerosol radiative properties using the TSI 3563 integrating nephelometer, *Aerosol Sci. Tech.*, 29, 57–69, 1998.

Anderson, T. L., Covert, D. S., Marshall, S. F., Laucks, M. L., Charlson, R. J., Waggoner, A. P., Ogren, J. A., Caldow, R., Holm, R. L., Quant, F. R., Sem, G. J., Wiedensohler, A., Ahlquist, N. A., and Bates, T. S.: Performance characteristics of a high-sensitivity, three-wavelength, total scatter/backscatter nephelometer, *J. Atmos. Ocean. Tech.*, 13, 967–986, 1996.

Andrews, E., Sheridan, P. J., Fiebig, M., McComiskey, A., Ogren, J. A., Arnott, P., Covert, D., Elleman, R., Gasparini, R., Collins, D., Jonsson, H., Schmid, B., and Wang, J.: Comparison of methods for deriving aerosol asymmetry parameter, *J. Geophys. Res.*, 111, D05S04, doi:10.1029/2004JD005734, 2006.

Beuttell, R. G. and Brewer, A. W.: Instruments for the measurement of the visual range, *J. Sci. Instr. Phys. Ind.*, 26, 357–359, 1949.

Bohren, C. F. and Huffman D. R.: *Absorption and Scattering of Light by Small Particles*, Wiley, New York, USA, 1983.

Buchholz, A.: Rayleigh scattering calculations for the terrestrial atmosphere, *Appl. Optics*, 34, 2765–2773, 1995.

Charlson, R. J., Porch, W. M., Waggoner, A. P., and Ahlquist, N. C.: Background aerosol light-scattering characteristics – nephelometric observations at Mauna-Loa-observatory compared with results at other remote locations, *Tellus*, 26, 345–360, 1974.

DeCarlo, P., Slowik, J., Worsnop, D., Davidovits, P., and Jimenez, J.: Particle Morphology and Density Characterization by Combined Mobility and Aerodynamic Diameter Measurements, Part 1: Theory, *Aerosol Sci. Tech.*, 38, 1185–1205, 2004.

Ecotech: Aurora 3000 User manual 1.3, November, 2009.

Heintzenberg, J.: The angular calibration of the total scatter/backscatter nephelometer, consequences and application, *Staub Reinhalt. Luft*, 38, 62–63, 1978.

Three-wavelength LED-based total scatter integrating nephelometer

T. Müller et al.

Title Page

Abstract

Introduction

Conclusions

References

Tables

Figures

⏪

⏩

◀

▶

Back

Close

Full Screen / Esc

Printer-friendly Version

Interactive Discussion



Three-wavelength LED-based total scatter integrating nephelometer

T. Müller et al.

Title Page

Abstract

Introduction

Conclusions

References

Tables

Figures

⏪

⏩

◀

▶

Back

Close

Full Screen / Esc

Printer-friendly Version

Interactive Discussion



- Heintzenberg, J. and Charlson, R. J.: Design and applications of the integrating nephelometer: A review, *J. Atmos. Ocean. Tech.*, 13, 987–1000, 1996.
- Heintzenberg, J., Wiedensohler, A., Tuch, T. M., Covert, D. S., Sheridan, P., Ogren, J. A., Gras, J., Nessler, R., Kleefeld, C., Kalivitis, N., Aaltonen, V., Wilhelm, R. T. and Havlicek, M.: Intercomparisons and aerosol calibrations of 12 commercial integrating nephelometers of three manufacturers, *J. Atmos. Ocean. Tech.*, 23, 902–914, 2006.
- Marshall, S. F., Covert, D. S., and Charlson, R. J.: Relationship between asymmetry parameter and hemispheric backscatter ratio – implications for climate forcing by aerosols, *Appl. Optics*, 34, 6306–6311, 1995.
- Massoli, P., Murphy, D. M., Lack, D. A., Baynard, T., Brock, C. A., and Lovejoy, E. R.: Uncertainty in Light Scattering Measurements by TSI Nephelometer: Results from Laboratory Studies and Implications for Ambient Measurements, *Aerosol Sci. Tech.*, 43, 1064–1074, 2009.
- Moosmüller, H. and Arnott, W. P.: Angular truncation errors in integrating nephelometry, *Rev. Sci. Instrum.*, 74, 3492–3501, 2003.
- Müller, T., Nowak, A., Wiedensohler, A., Sheridan, P., Laborde, M., Covert, D. S., Marinoni, A., Imre, K., Henzing, B., Roger, J. C., dos Santos, S. M., Wilhelm, R., Wang, Y. Q., and de Leeuw, G.: Angular Illumination and Truncation of Three Different Integrating Nephelometers: Implications for Empirical, Size-Based Corrections, *Aerosol Sci. Tech.*, 43, 581–586, 2009.
- Wex, H., Neusüß, C., Wendisch, M., Stratmann, F., Koziar, C., Keil, A., Wiedensohler, A., and Ebert, M.: Particle scattering, backscattering, and absorption coefficients: An in situ closure and sensitivity study, *J. Geophys. Res.*, 107(D21), 8122, doi:10.1029/2000JD000234, 2002.
- Wang, S. C. and Flagan, R. C.: Scanning electrical mobility spectrometer. *J. Aerosol Sci.*, 20, 1485–1488, 1989.

Three-wavelength LED-based total scatter integrating nephelometer

T. Müller et al.

Table 1. Parameters for truncation and non-Lambertian illumination correction functions. Correction functions are given for TSI model 3565 and Aurora 3000 nephelometers.

Nephelometer	α_1	α_2	β_1	β_2	γ_1	γ_2
TSI 3563 ¹	7°	170°	1.175	1.005	73.86	32.84
Aurora 3000	10°	171°	1.190	1.01	70.25	39.99

¹ Parameters were derived from sensitivity functions published in Müller et al. (2009).

[Title Page](#)
[Abstract](#)
[Introduction](#)
[Conclusions](#)
[References](#)
[Tables](#)
[Figures](#)
[⏪](#)
[⏩](#)
[◀](#)
[▶](#)
[Back](#)
[Close](#)
[Full Screen / Esc](#)
[Printer-friendly Version](#)
[Interactive Discussion](#)


Three-wavelength LED-based total scatter integrating nephelometer

T. Müller et al.

[Title Page](#)[Abstract](#)[Introduction](#)[Conclusions](#)[References](#)[Tables](#)[Figures](#)[⏪](#)[⏩](#)[◀](#)[▶](#)[Back](#)[Close](#)[Full Screen / Esc](#)[Printer-friendly Version](#)[Interactive Discussion](#)

Table 2. Results of regression analysis ($\sigma_{\text{Aurora 3000}} = m\sigma_{\text{TSI 3563}} + b$ and the coefficient of determination R^2) of the Aurora 3000 and TSI 3563 for total scattering (ts) and backscattering (bs). Directly measured values as well as angular sensitivity corrected values are shown. Wavelengths are B = 450 nm, G = 525 nm, and R = 635 nm. Values are given for (a) ammonium sulphate and (b) ambient air.

(a) Ammonium sulphate						
	ts, B	ts, G	ts, R	bs, B	bs, G	bs, R
without angular sensitivity correction						
slope (m)	0.94	0.96	0.94	0.95	1.04	1.13
intercept (b)	0.51	0.64	0.94	0.46	0.61	0.88
R^2	0.998	0.995	0.996	0.993	0.991	0.988
with angular sensitivity correction						
slope (m)	0.96	0.98	0.95	0.93	1.01	1.11
intercept (b)	0.56	0.68	0.97	0.43	0.57	0.81
R^2	0.998	0.995	0.996	0.993	0.991	0.998
(b) Ambient air						
	ts, B	ts, G	ts, R	bs, B	bs, G	bs, R
without angular sensitivity correction						
slope (m)	0.96	0.98	0.93	1.04	1.05	0.98
intercept (b)	1.38	1.08	0.45	-0.07	-0.14	0.06
R^2	0.997	0.997	0.997	0.994	0.994	0.995
with angular sensitivity correction						
slope (m)	0.99	1.01	0.95	1.01	1.03	0.96
intercept (b)	1.04	0.86	0.26	-0.11	-0.16	-0.03
R^2	0.998	0.997	0.997	0.993	0.994	0.994

Three-wavelength LED-based total scatter integrating nephelometer

T. Müller et al.

Title Page

Abstract

Introduction

Conclusions

References

Tables

Figures

⏪

⏩

◀

▶

Back

Close

Full Screen / Esc

Printer-friendly Version

Interactive Discussion



Table 3. Ångström exponents for two wavelength pairs and angular sensitivity corrected total and backscattering, respectively. Given are the median and 10th and 90th percentiles for two wavelength pairs and total and backscattering, respectively.

wavelengths pair [nm]	TSI 3565				Aurora 3000			
	total scattering		backscattering		total scattering		backscattering	
	450/525	525/635	450/525	525/635	450/525	525/635	450/525	525/635
median	2.41	2.78	1.64	1.59	2.28	2.79	1.48	1.36
10th percentile	2.37	2.74	1.50	1.50	2.24	2.74	1.35	1.17
90th percentile	2.46	2.83	1.74	1.73	2.32	2.84	1.62	1.52

Three-wavelength LED-based total scatter integrating nephelometer

T. Müller et al.

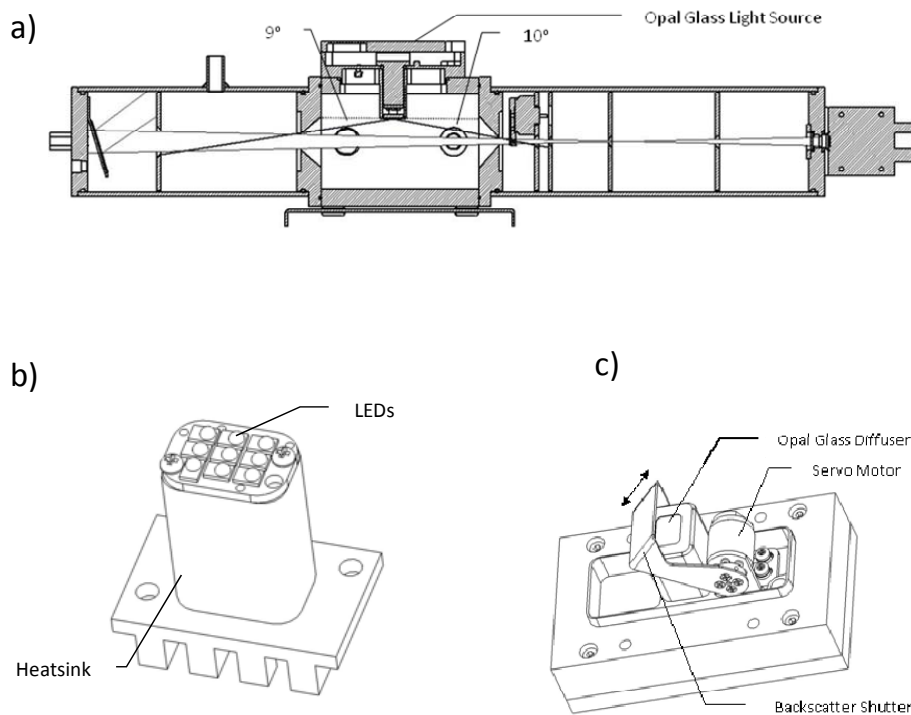


Fig. 1. Sketch of the Aurora 3000. **(a)** Sensing volume and indicated truncation angles. **(b)** Arrangement of LEDs. **(c)** Light source with motor driven backscatter shutter.

[Title Page](#)
[Abstract](#)
[Introduction](#)
[Conclusions](#)
[References](#)
[Tables](#)
[Figures](#)
[◀](#)
[▶](#)
[◀](#)
[▶](#)
[Back](#)
[Close](#)
[Full Screen / Esc](#)
[Printer-friendly Version](#)
[Interactive Discussion](#)

**Three-wavelength
LED-based total
scatter integrating
nephelometer**

T. Müller et al.

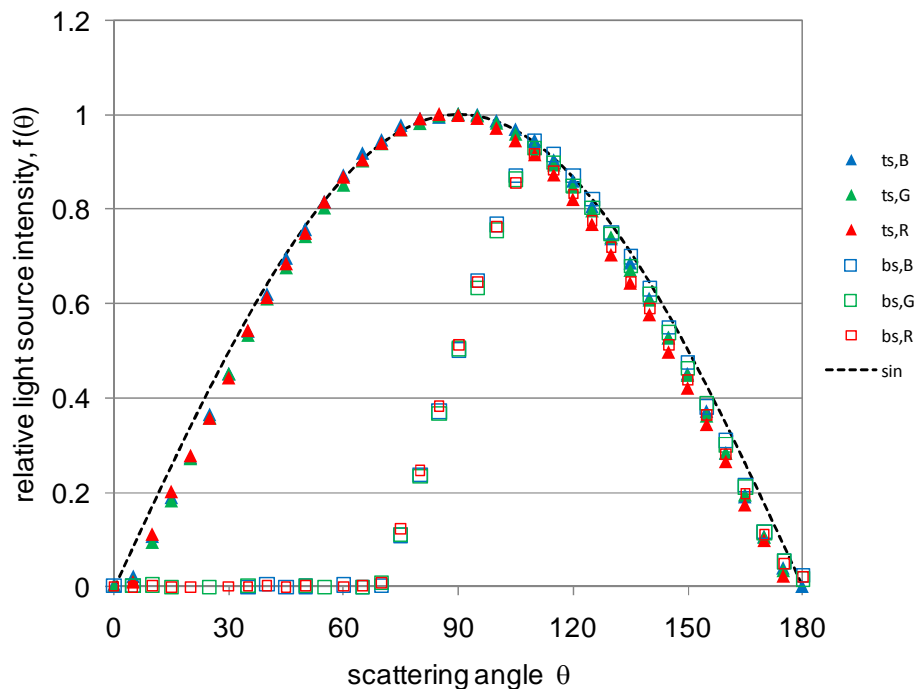


Fig. 2. Measured angular intensity functions for nephelometer model Aurora 3000. The wavelengths are indicated by B (450 nm), G (525 nm), and R (635 nm), respectively. Total scattering and backscattering are indicated by ts and bs respectively. For comparison purposes, the total angular intensity functions have been normalized.

[Title Page](#)[Abstract](#)[Introduction](#)[Conclusions](#)[References](#)[Tables](#)[Figures](#)[◀](#)[▶](#)[◀](#)[▶](#)[Back](#)[Close](#)[Full Screen / Esc](#)[Printer-friendly Version](#)[Interactive Discussion](#)

Three-wavelength LED-based total scatter integrating nephelometer

T. Müller et al.

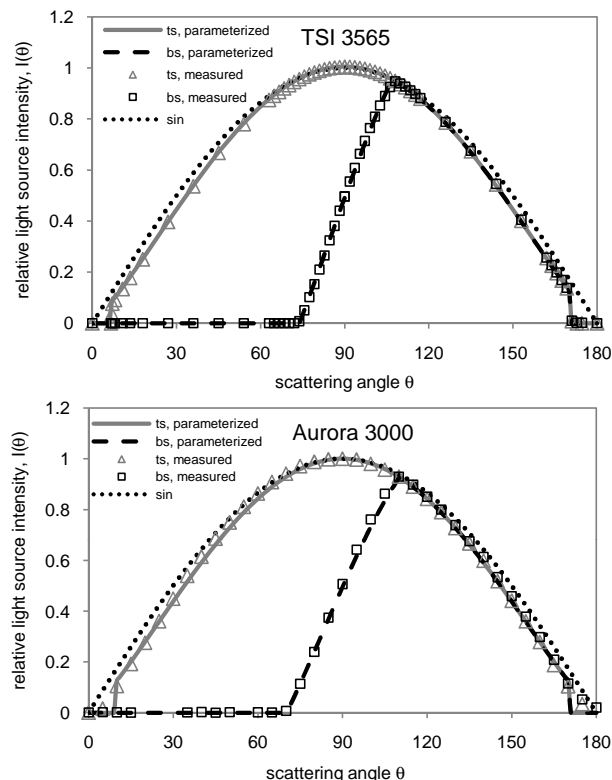


Fig. 3. Measured and parameterized angular intensity functions, $f(\theta)$, including forward and backward truncation for the TSI 3563 (upper panel, data are taken from Anderson et al., 1996) and Aurora 3000 (lower panel). For the Aurora 3000 the average of all three wavelengths is shown. For comparison purposes, the total scattering illumination function (ts) has been normalized to unity at 90° scattering angle. The backward scattering illumination function (bs) was adjusted to match the total scattering function at 110° .

[Title Page](#)
[Abstract](#)
[Introduction](#)
[Conclusions](#)
[References](#)
[Tables](#)
[Figures](#)
[◀](#)
[▶](#)
[◀](#)
[▶](#)
[Back](#)
[Close](#)
[Full Screen / Esc](#)
[Printer-friendly Version](#)
[Interactive Discussion](#)

Three-wavelength LED-based total scatter integrating nephelometer

T. Müller et al.

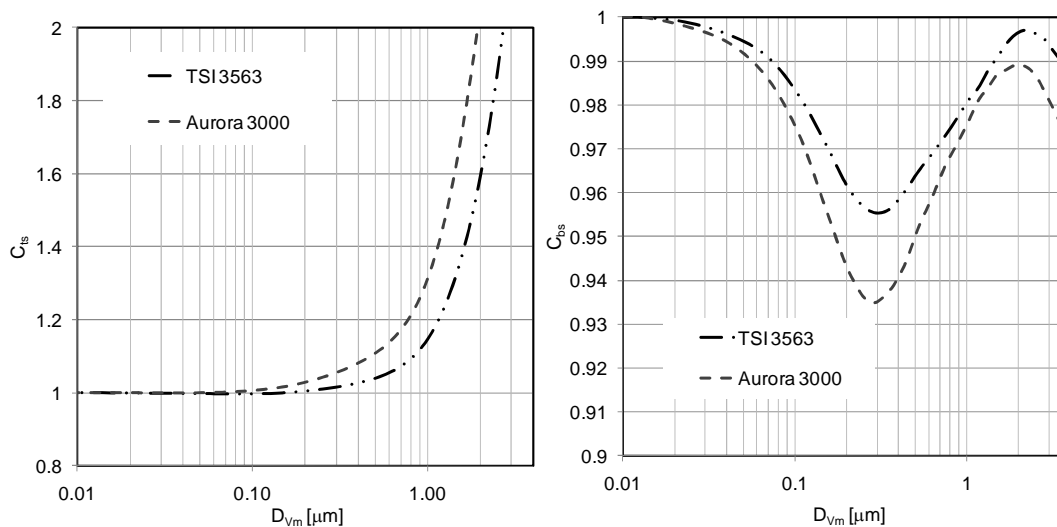


Fig. 4. Angular sensitivity correction factors for total scattering (left panel) and backscattering (right panel) versus the volume median diameter of a lognormal volume size distribution with geometric standard deviation 1.6. The refractive index of the aerosol was chosen to be $1.53 - 0.01i$. The wavelength for calculating correction factors were 525 and 550 nm for Aurora 300 and TSI 3563, respectively.

Title Page

Abstract

Introduction

Conclusions

References

Tables

Figures

⏪

⏩

◀

▶

Back

Close

Full Screen / Esc

Printer-friendly Version

Interactive Discussion

**Three-wavelength
LED-based total
scatter integrating
nephelometer**

T. Müller et al.

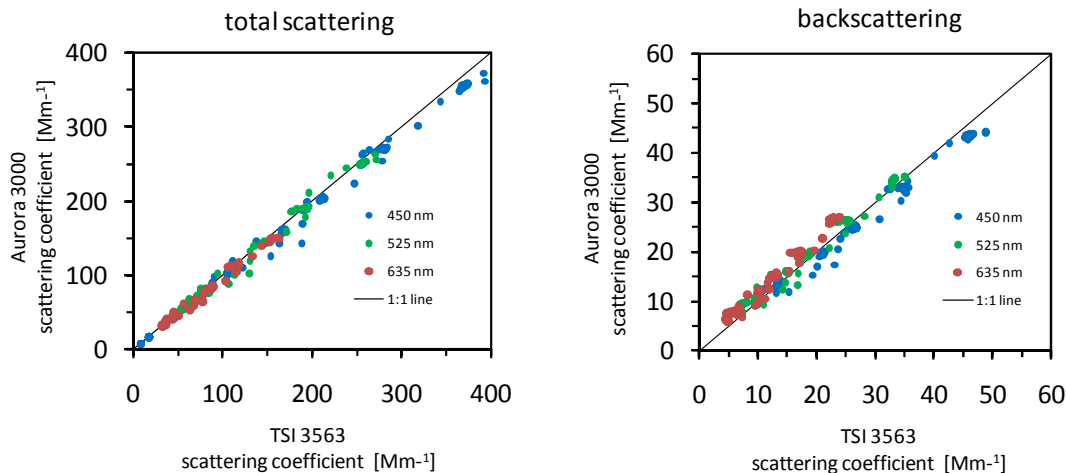


Fig. 5. Correlation between total scattering coefficients measured with the TSI 3565 and Aurora 3000, respectively. The left panel shows the correlation for total scattering coefficients including truncation correction. Wavelengths for TSI 3563 were adjusted to 450, 525, and 635 nm. The right panel is similar to the left panel but for backscattering coefficients.

**Three-wavelength
LED-based total
scatter integrating
nephelometer**

T. Müller et al.

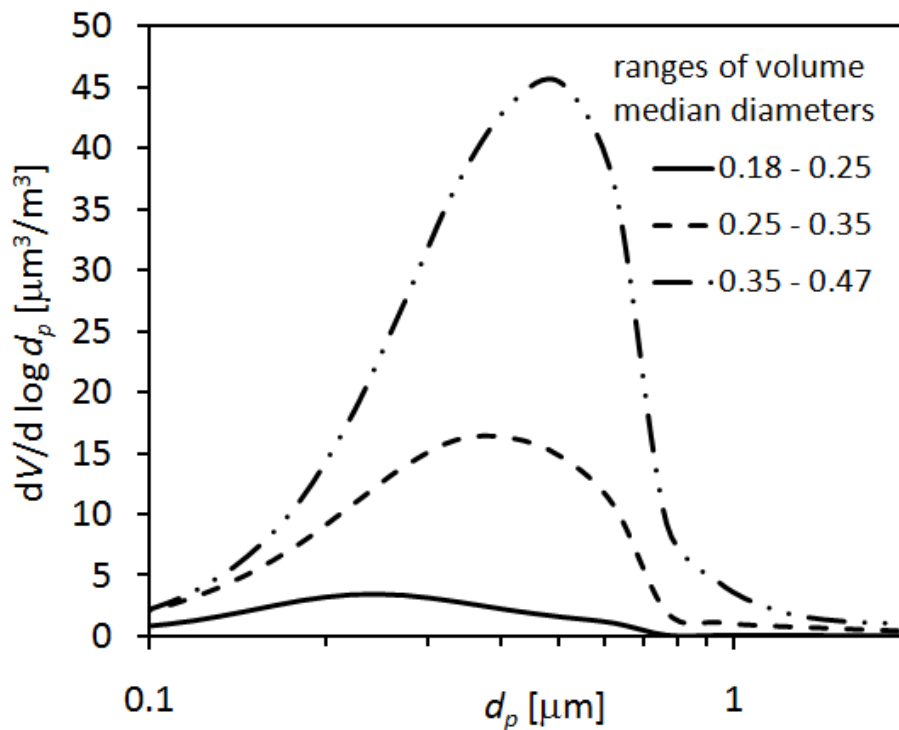


Fig. 6. Average particle volume size distributions classified for three ranges of volume median diameters.

[Title Page](#)[Abstract](#)[Introduction](#)[Conclusions](#)[References](#)[Tables](#)[Figures](#)[◀](#)[▶](#)[◀](#)[▶](#)[Back](#)[Close](#)[Full Screen / Esc](#)[Printer-friendly Version](#)[Interactive Discussion](#)

**Three-wavelength
LED-based total
scatter integrating
nephelometer**

T. Müller et al.

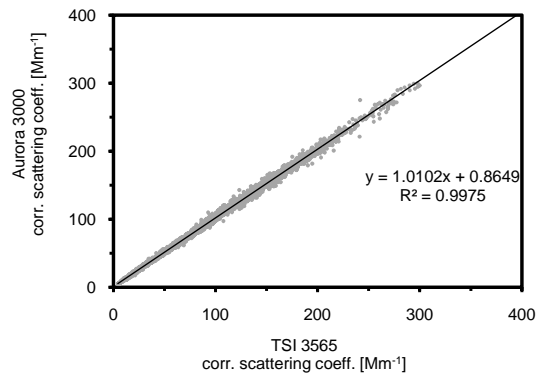
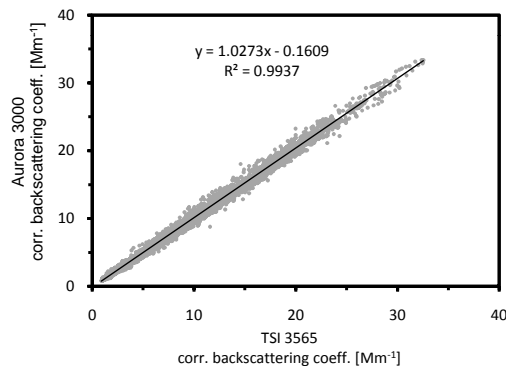
a) total scattering**b) backscattering**

Fig. 7. Panel (a): Correlation between total scattering coefficients measured with the TSI model 3565 and Aurora 3000, respectively. Panel (b) shows the correlation for backscattering coefficients. Total scattering and backscattering at 525 nm were corrected for angular sensitivities. TSI 3525 scattering coefficients were adjusted to wavelength 525 nm using an interpolation based on the Ångström exponents.

Title Page

Abstract

Introduction

Conclusions

References

Tables

Figures

◀

▶

◀

▶

Back

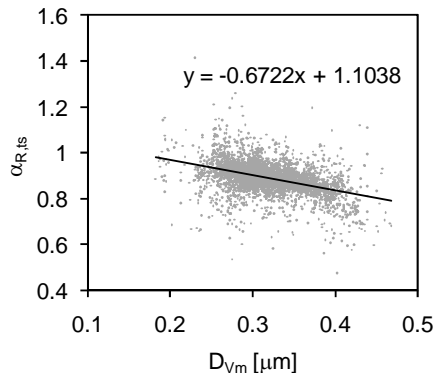
Close

Full Screen / Esc

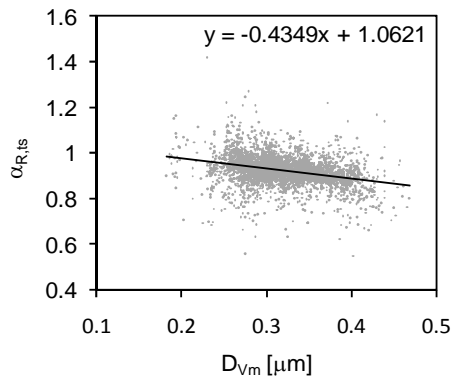
Printer-friendly Version

Interactive Discussion

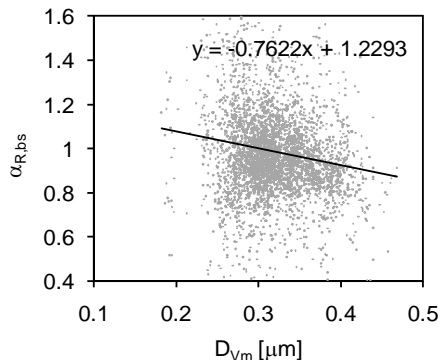
a) total scattering without corrections



b) total scattering with corrections



c) backscattering without corrections



d) backscattering with corrections

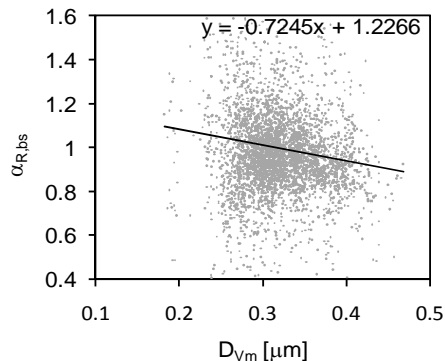


Fig. 8. Ratios of Ångström exponents (α_R), defined by Ångström exponents from the Aurora 3000 divided by Ångström exponents from the TSI 3565. Panel (a) and (b) show ratios for uncorrected and sensitivity corrected total scattering. Ratios for uncorrected and sensitivity corrected backscattering are shown in panels (c) and (d).